Variations in the electric potential of a metal nanoparticle on a dielectric

© A.V. Ankudinov[1], A.S. Vlasov[1], M.S. Dunaevskiy[1], V.Yu. Axenov[1], I.V. Ilkiv[2], A.V. Malevskaya[1], V.D. Rodin[1], A.S. Tschenin[1], A.M. Mintairov[1]

[1] Ioffe Institute,
194021 St. Petersburg, Russia
[2] St. Petersburg State University,
199034 St. Petersburg, Russia

E-mail: alex_ank@mail.ru, alexander.ankudinov@mail.ioffe.ru

Received November 5, 2025
Revised December 2, 2025
Accepted December 8, 2025

Using scanning Kelvin probe microscopy under room conditions, flickering of the surface potential signal over single 20−70 nm Au particles in the micro apertures of a perforated Au contact of a flat capacitor with the GaIn−pSi−SiO_2−Au structure was investigated. It was found that the flickering amplitude increases with decreasing particle size and probe-sample distance. The relationship between the flickering and thermal fluctuations of the particle potential, as well as other sources, was analyzed. Calibration of the surface potential signal on a nanoscale potential flicker source made it possible to identify the response to elementary charge jumps in the experimental data.

Keywords: scanning probe microscopy, metallic nanoparticles, elementary electric charge, thermal noise.

DOI: 10.61011/SC.2025.10.62871.8749

1. Introduction

At room temperature, a metal particle with a size of 100 nm has a RMS amplitude of thermal charge noise that becomes less than $e = 1.602 \cdot 10^{-19}$ C. The quantum of electric charge e was determined with almost modern precision by Millikan, controlling the speed of movement of micron oil droplets in the gravitational field by the vertical electric field [1]. Charge quantization is an empirical law, and in the last century, the possibility of detecting a fractional (relative to an electron) charge of a free quark was discussed [2]. Experiments were also conducted [3]: submillimeter diamagnetic particles suspended in a magnetic field were studied, which, as it was found, occupied discrete equilibrium positions corresponding to elementary charge surges on them when the electric field was turned on. Charge fluctuations of metallic nanoparticles can be investigated by measuring their potential using scanning Kelvin probe microscopy (SKPM) [4]. The purpose of such studies is not only to test the law of charge quantization, but also to search for calibrated nanometer-sized potential sources for SKPM verification.

We used SKPM in the mode of amplitude modulation (AM) to measure the electrical potential of Au-nano particles [5]. Colloidal particles (see Figure 1) were deposited on a special sample. It consisted of a flat silicon-based capacitor with a thick, $d \approx 1.4\,\mu$m, thermal oxide and a perforated upper electrode (Figure 2, a). The temporal fluctuations of the potential of an Au particle located on the dielectric surface inside the micro-hole in the electrode were measured in the zero edge field of the capacitor or by unfolding the voltage on the capacitor plates in order to change the surface charge of the micro-hole with an accuracy of a fraction of the electron charge. Data are presented on single particles with a diameter in the range of 20−70 nm, which fluctuate with an amplitude proportional to the jumps in the particle potential when the charge changes by $1e$. Using calculations of the particle capacity using the „sphere on a dielectric“ model, the results obtained can be reconciled with thermal potential fluctuations.

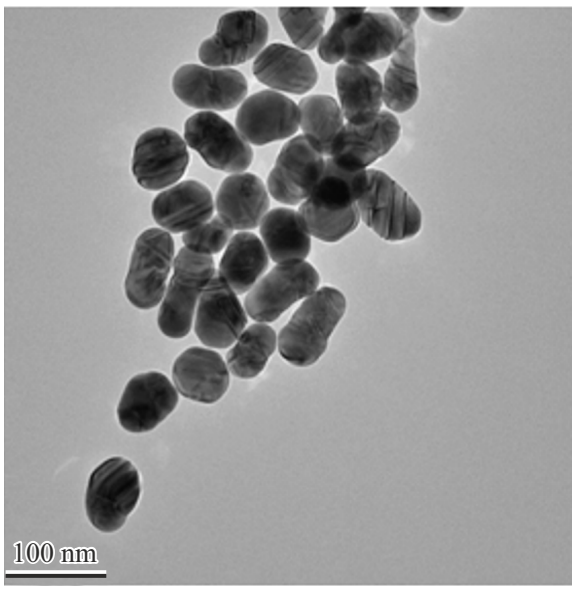

Figure 1. Transmission electron microscopy of colloidal Au particles used in this study. Average image width, length, „ellipticity“ particles: 47 ± 7, 69 ± 10 nm, 0.69 ± 0.13.

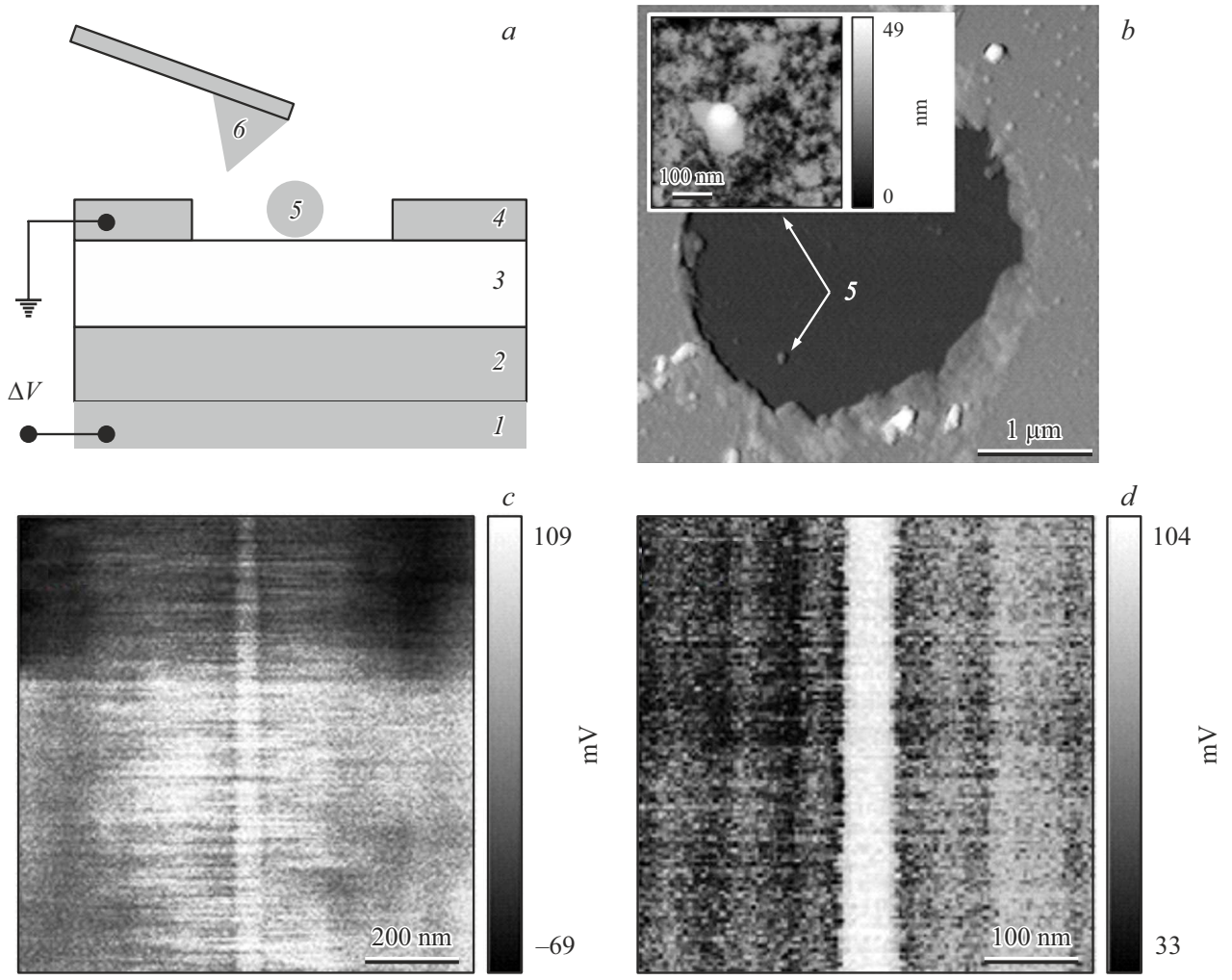

Figure 2. *a* — experimental scheme: solid GaIn contact (*1*), *p*-Si (*2*), thermal oxide $d \approx 1.4\,\mu$m (*3*), perforated Au contact (*4*), particles (*5*), cantilever (*6*). *b* — AFM image of the Au contact area with a single Au particle in the hole $D \approx 3\,\mu$m; a gray scale image with the best resolution is shown in the insert. SP signal: *c* — 36-nanometer particle in hole; *d* — 26-nanometer particle on contact. Measurement parameters: repeated scanning of a single line with a particle in the middle, probe distance−surface $h = 20$ nm; number of lines per frame and scan time, with: *c* — 201 and 473, *d* — 128 and 294; cantilever 2 (see Table).

SKPM studies of the charge states of nanoparticles are being conducted quite actively [6–9]. In contrast to our measurements, particles of an order of magnitude smaller in size are taken, with Coulomb energy (the electrostatic energy of a particle with charge $1e$) significantly exceeding the thermal energy. Instead of single particles on a micron-thick insulator, the arrays of particles with a characteristic density $10^3\,\mu\text{m}^{-2}$, separated from the conductive contact (substrate) by a tunnel-transparent [6–8] dielectric layer are studied.

Charge fluctuations of metal islands have been actively studied using single-electron transistors [10–13], which are ultra-sensitive electrometers. Such experiments require low temperatures. In addition, in the measured fluctuations, the contribution of noise with a spectral density $\sim 1/f$ significantly exceeds the background shot noise of the transistor [11–13].

2. Sample preparation

The scheme of SKPM studies of the charge states of a metal nanoparticle is shown in Figure 2, *a*. The upper, perforated electrode of the capacitor structure has holes of different diameters, $D = 1.5$, 2, 3 and $4\,\mu$m. When a voltage of ΔV is applied to the capacitor (Figure 2, *a*), the hole receives a charge no greater than $\Delta Q = \varepsilon\varepsilon_0\pi D^2\Delta V/4d$ (for SiO_2 $\varepsilon = 4$). For example, $\Delta V = 1$ mV creates $\Delta Q \approx 0.3$, 0.5, 1.1 and $2.0\,e$ in the named holes. Due to this, it is possible to smoothly affect the charge of the metal particle in the hole. Getting a single particle into the micro-hole seems to be optimal for measurements.

Gold nanoparticles from BBI solutions with a narrow size distribution were used. The concentration of particles in aqueous colloids stabilized with citrate ions was selected depending on their characteristic size and, for example,

Data of SKPM–measurements of Au particles*

Particle No.	Cantilever	R, nm	h, nm	σ_0, mV	$\sigma_0(0)$, mV
1	1. HAFM/W_2C; 6N/m	11	20	6.3	17.8
	2. NSC36/Pt; 1.6N/m		20	9.3	26.2
2	3. NSC36/Pt; 0.7N/m	17	10	10.7	17.0
3	4. CSG30/Pt; 0.4N/m	17	15	7.1**	13.4
4	5. CSG30/Pt; 0.5N/m	18	20	3.0	6.3
	2. NSC36/Pt; 1.6N/m		20	5.3	11.2
			20	9.1	18.2
	6. NSC36/Pt; 1.1N/m		25	6.4	15.3
			20	7.2	15.2
			15	7.9	14.5
			5	12.9	16.5
5	3. NSC36/Pt; 0.7N/m	24	8	9.4	12.5
6	7. NSC36/Pt; 1.1N/m	34	30	4.8	9.0

Note. * The radius of the particle, R; the probe-sample distance when registering the surface potential signal, h; the RMSV of the signal at a height of h above the particle in the zero edge field of the capacitor, σ_0; calculation of $\sigma_0(0) = \sigma_0(R+h)/R$. ** Average value, $(\sigma_- + \sigma_+)/2$.

was $9 \cdot 10^{10}$units/ml for 40-nanometer and 8 times lower for 80-nanometer particles. A drop of colloid ($80\,\mu$l) was deposited on the surface of the perforated electrode for a period of 30 seconds or longer, which was then removed by a jet of compressed nitrogen.

Visualization of the surface relief of samples in scanning electron and atomic–force microscopes (SEM and AFM) after application of colloidal solutions showed that the probability of deposition of Au particles on the surface of SiO_2 in the contact holes is significantly lower than on its metallized surface. The exposure time of the colloid droplet on the sample had to be increased to deposit the particles into the holes, up to the moment of complete drying.

The search for micro-holes with single particles on the sample took a long time. A successful result, with a single Au particle with a height of 36 nm (later measured in AFM, we assume the particle height to be equal to its diameter) in the upper contact hole with an area of $\sim 7\,\mu m^2$, is shown in Figure 2, *b* and on insert. In the upper-right corner of the frame, on the contact, similar particles are visible, the surface density of which is 2 orders of magnitude higher.

Attempts have been made to optimize the deposition technology. Before applying the colloid, the samples were processed in an IntlVac Nanoquest II facility system using Kaufman–Robinson ion source. A perpendicularly directed electron beam was used to neutralize the charged ion beam. The procedure was performed within 60 seconds after reaching a vacuum in the working chamber of at least 10^{-7} Torr. The argon flow of the ion cannon was 26 standard cm^3/min at an accelerating voltage of 200 V. The treatment increased the number of holes with a single particle, but formed a long-lived conductive channel on the surface of the dielectric, removing charge from the particles. Such a channel completely shielded the internal field of the capacitor, which was revealed by the insensitivity of the surface potential (SP) SKPM signal in the hole area to voltage variations on the lower capacitor plate (Figure 2, *a*) with the upper plate grounded.

3. Measurement results and calculations

Figure 2, *c* and *d* show the results of a study of the electrical potential of single particles: a 36-nanometer particle on an insulating surface inside the three-micron hole of the upper electrode of the capacitor structure and a 26-nanometer particle on a conductive surface outside the hole. A two-pass SKPM mode was used. First, the relief signal was measured, and then at a given distance h from the sample, the SP signal was recorded along the measured trajectory. Only X-sweep of the scanner was involved, the frame heights are responsible for the time spent on such scanning: pp. 473 and 294. Both contacts of the sample are grounded, and there is a zero field in the capacitor.

The image of the SP signal in Figure 2, *c* shows a band of instability, flickering potential with a narrow ~ 50 nm light contrast strip in the middle, reflecting the signal growth above the 36-nanometer particle. Since the flickers of the potential fade to the left and right of the particle, it is their source. The width of the flicker band characterizes the SP response to the peak potential above the particle, namely, the cross section of the probe's hardware function (PHF) in the AM SKPM mode [5,14] is a plane across the cantilever. The main contribution to the observed broadening is provided by the electrostatic interaction of the particle with the faces of the pyramidal probe. Using only the Y-sweep of the scanner, it is possible to study the section of the PHF plane along the cantilever.

In the image of the SP signal in Figure 2, *d*, only a narrow vertical light contrast strip of the signal above the 26-nanometer particle is observed. Unlike in Figure 2, *c*, potential flickers are not detected at least in the time range from 2–294 s (line scan frequency ≈ 0.5 Hz).

The studies also showed that the potential of an Au particle does not „flicker“ if it is: a particle in the agglomerate; a single particle in the micro-hole of a sample treated with argon ions before applying the colloid; a single particle on the surface of GaAs and Si; a single particle on the surface of a thick, $d \approx 1.4\,\mu$m, thermal silicon oxide in the absence of a perforated upper contact. As for the 26-nanometer particle, in the first three cases, the reason is the conductive environment, which quickly removes charge from the particle. In the latter case, the absence of flicker seems to indicate that the manufacturing process of the upper contact may reduce the insulating properties of the thermal oxide surface.

The profiles of the SP signal (time-dependent) over a 36-nanometer particle and a 26-nanometer particle (Figu-

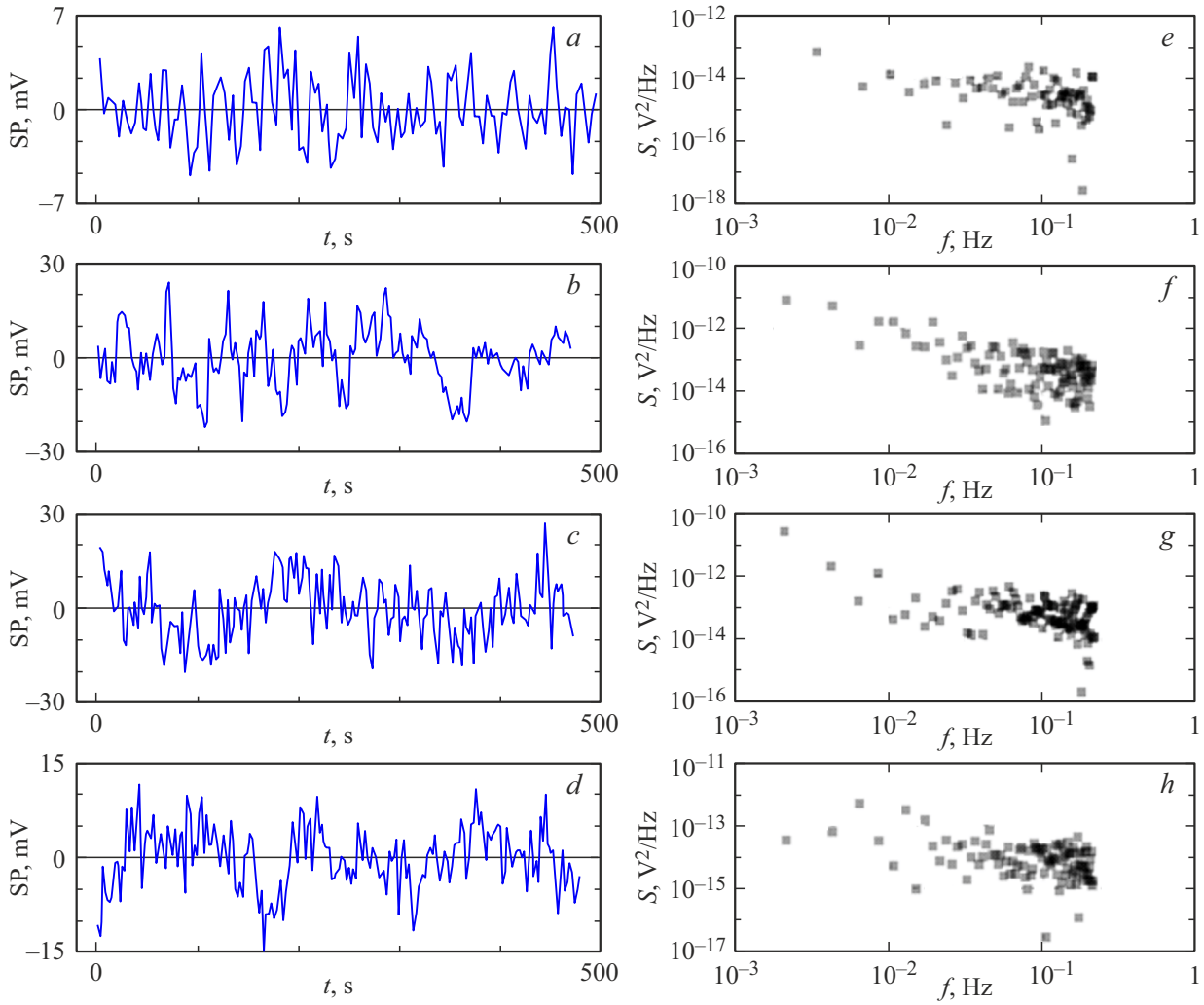

Figure 3. Temporal fluctuations of the SP signal over particles of different sizes on the conductor and insulator and their corresponding spectra in the zero field: 26 nm on Au (*a* and *e*); 22 nm on SiO_2 (*b* and *f*), 36 nm on SiO_2 (*c* and *g*), 68 nm on SiO_2 (*d* and *h*) (particles No. 1, 4 and 6 in the Table). Cantilevers: *a*–*c* — 2, *d* — 7 (see Table). The profile of *a* and the spectrum of *e* characterize the intrinsic noise of SKPM.

re 2, *c* and *d*) after subtracting the curve of the 3rd order are shown in Figure 3, *c* and *a*. At zero field of the capacitor, the particle at the contact has a root mean square variation (RMSV) of the potential $\sigma_0 = 2.4$ mV, and the particle in the hole $\sigma_0 = 9.1$ mV (No. 4, see Table). The first value characterizes the instrumental noise level of the SP signal. The flickering potential on a 36-nanometer particle is 4 times greater than the noise.

Figure 3, *b* and *d* show the profiles of the SP signal over single 22-nanometer and 68-nanometer particles on the surface of SiO_2 in the contact holes. For them $\sigma_0 = 9.3$ and 4.8 mV (No. 1 and 6, see Table).

In terms of the amplitude of the flicker of particles on the surface of SiO_2 (Figure 3, *b*–*d*), the noise above the particle on the Au contact is several times higher (Figure 3, *a*). If the flickering reflects the activation process of the particle charge jump, then the smallest particles should flicker less often, with a higher capture energy of one electron.

This is observed in Figure 3, *b*–*d*, as well as in the power density spectra of the signal (Figure 3, *f*–*h*) (Fourier-transformations of raw SP signal profile data, without subtracting the 3rd order curve). In particular, the spectra of 22-, 36-, and 68-nanometer particles have an average slope tangent: −1.2, −0.8 and −0.6 respectively. The slope of the spectrum, however, can be distorted by low-frequency hardware drifts.

The manifestation of this drift can be seen in Figure 2, *c*. In the upper part of the frame, the contrast changes abruptly both above and away from the particle. Since the measurements were not carried out under ultrahigh vacuum conditions, the adsorption-desorption of contaminants onto the probe and sample can change the contact potential difference. In addition, the light from the 650-nanometer laser used in the optical cantilever deflection detection system is absorbed in silicon, which can change the electric field at the Si–SiO_2 interface.

Let us estimate the amplitude of the thermal fluctuations of the potential of a conducting particle on an insulator. For simplicity, as in Ref. [7], we will consider them spheres with radius R.

According to transmission electron microscopy data (Figure 1), the Au particles used are closer in shape to ellipsoids with average ellipticity $k \approx 0.7$. The capacity of the ellipsoid of rotation with a short axis is R: $4\pi\varepsilon_0 R \times [k^{-2}-1]^{1/2}/\ln(k^{-1}+[k^{-2}-1]^{1/2})$ [15]. The difference from the capacity of the sphere $4\pi\varepsilon_0 R$ is 1.14 times, which gives a measure of the proximity of the selected approximation to reality.

A sphere with a charge Q lying on a dielectric (SiO_2, $\varepsilon = 4$) creates a potential over the dielectric, $z \geq -R$ (see [16–18] and *Appendix*, F. (A.9):

$$\varphi = \frac{(\varepsilon-1)}{4\pi(\varepsilon+1)\varepsilon_0 \ln[(\varepsilon+1)/2]}\, Q \times \left(\frac{1}{|r|}+\sum_{n=2}^{\infty}\frac{K^{n-1}}{|n\mathbf{r}+(n-1)R\mathbf{e}_Z|}-\sum_{n=1}^{\infty}\frac{K^n}{|n\mathbf{r}+(n+1)R\mathbf{e}_Z|}\right), \quad (1)$$

where $K = (\varepsilon-1)/(\varepsilon+1)$.

In the experiment, the potential is measured at a height of h above the sample surface. A sphere with a charge of $1e$ creates a potential at a height of h above itself:

$$\varphi_e(h) = \frac{(\varepsilon-1)}{4\pi(\varepsilon+1)\varepsilon_0 \ln[(\varepsilon+1)/2]}\, e \times \left(\frac{1}{R+h}-\sum_{n=1}^{\infty}\frac{K^n h}{[(2n+1)R+nh][(2n+1)R+(n+1)h]}\right). \quad (2)$$

The corresponding Coulomb energy is as follows:

$$\Phi_e = \frac{e\varphi_e(0)}{2} = \frac{e^2}{2C} = \frac{(\varepsilon-1)e^2}{8\pi(\varepsilon+1)\varepsilon_0 R \ln[(\varepsilon+1)/2]}. \quad (3)$$

For the studied particles (see Table) Φ_e/e lies in the range 10−50 mV.

Fluctuations in the potential of a conducting particle on a dielectric can be determined not only by variations in its charge (intrinsic noise), but also by the behavior of external charges in the dielectric (induced noise).

External charges in the dielectric, trapped at distances from the particle $\gg R$, create a far field E_1, which is shielded in the metal by an induced charge — a dipole. The corresponding addition to the particle potential is $\sim E_1 R$. The charge Q_2 on a single trap near a particle acts with a near field E_2. The shielding E_2 induces the difference of potentials $\sim Q_2/R$ on the particle.

To reduce the parasitic contribution of external charges to the potential of a particle, a dielectric with a low trap density is needed, i. e., with a small volume charge and, as a result, E_1. If the traps are deep, with energy significantly higher than the thermal and charge capture energy of the particle itself, then the role of E_2 will be reduced.

Let us estimate the change in the potential of the particle $\Delta\varphi$ due to its polarization by the edge field of the capacitor $\mathbf{E}$. A conducting sphere introduced into the field $\mathbf{E}$ at point $\mathbf{r}$ will create a potential $\varphi_d = (\mathbf{E}, \mathbf{r})(R/r)^3$ [18]. At height h above it $|\Delta\varphi| = |E|h(3R^2+3Rh+h^2)/(R+h)^2$. The field at the edge of the capacitor is smaller than inside: $|E| < |\Delta V|/d$. Therefore, for example, $R = h = 20$ nm: $|\Delta\varphi| < |\Delta V|/40$. Thus, $\Delta\varphi$ does not exceed several mV if $\Delta V \approx 100$ mV.

A conducting particle $Q = ne$ with a charge uniformly distributed over the surface has electrostatic energy Φ_n:

$$\Phi_n = n^2\Phi_e. \quad (4)$$

Considering $\langle n\rangle = 0$, the particle is neutral on average, and its energy $\langle\Phi\rangle$, equal to thermal [19], is written as:

$$\langle\Phi\rangle = \langle n^2\rangle\Phi_e = \sigma_{nC}^2\Phi_e = \frac{k_B T}{2}. \quad (5)$$

Using (5) and the general ratio for the RMS potential at altitude h

$$\sigma_\varphi = \sigma_n\varphi_e(h), \quad (6)$$

we obtain for the RMS potential $\sigma_{\varphi C}$ without taking into account the discreteness of the levels:

$$\sigma_{\varphi C} = \varphi_e(h)\sqrt{\frac{k_B T}{e\varphi_e(0)}}. \quad (7)$$

Taking into account the discreteness using the Gibbs distribution [19], we determine the RMS of the number of electrons per particle, σ_{nQ}, and the associated $\sigma_{\varphi Q}$:

$$\sigma_{\varphi Q} = \sigma_{nQ}\varphi_e(h),$$

$$\sigma_{nQ} = \sqrt{\sum_{-\infty}^{+\infty} n^2 \exp\left(-n^2\frac{\Phi_e}{k_B T}\right) \Big/ \sum_{-\infty}^{+\infty}\exp\left(-n^2\frac{\Phi_e}{k_B T}\right)}. \quad (8)$$

Since $\Phi_e/k_B T \approx 1$, both rows converge very quickly at the root.

In Figure 4, solid and dotted, C and Q, the curves show the dependencies of $\sigma_{\varphi C}$ (7) and $\sigma_{\varphi Q}$ (8) on the radius R of the particle calculated for $h = 0$ and $\varepsilon = 4$. For large particles, $R > 15$ nm ($\Phi_e < k_B T$), the curves coincide. With decrease of R C-dependence increases monotonously, and Q-dependence passes through a maximum at $R \approx 8$ nm ($\Phi_e \approx 2.35 k_B T$), after which it quickly decreases to zero.

In Figure 4 circles show the measurement results. For each of the six particles, the average values of $\sigma_0(0)$ are displayed in the right column of the Table. The value $\sigma_0(0)$ was calculated from the measured σ_0 in the approximation of the inverse dependence of the potential on the distance to the center of the particle. The approach is justified. The series in dependence (2) converges quickly, since $K = 0.6$. The inverse relationship was observed in the experiment (see Table, particle No. 4, cantilever 6).

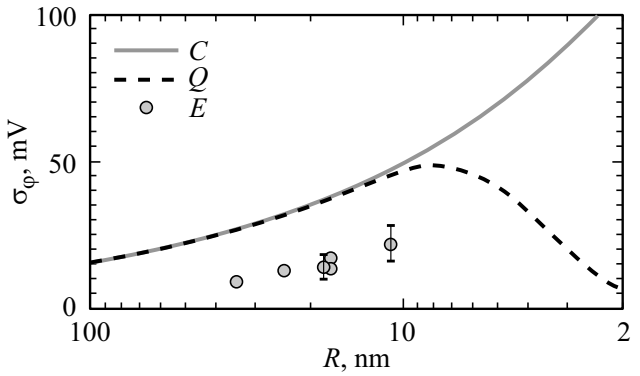

Figure 4. Calculated values without taking into account, C, and taking into account the discreteness of energy levels, Q, thermal potential fluctuations as a function of the radius R of a metal sphere lying on an insulator with $\varepsilon = 4$; measurement results in the zero edge field of the capacitor, E.

In Figure 4, the readings of measurements and calculations increase with a decrease of R. Agreement with the theory — qualitative, AM SKPM underestimates fluctuations: ~ 3 times on the largest particle (No. 6) and in ~ 2 times on the smallest (No. 1). The statistical significance of the data from these extreme points is low. The problem is that repeated scanning, as a rule, led to the capture of a particle loosely bound to the substrate onto the probe. However, it is worth emphasizing that the capacitive coupling of the probe tip with a large particle is stronger, and under equal conditions, the underestimation of the potential above it should be less. The measurement conditions were not equal — different cantilevers were used: by 10 nm more for 6 h than for 1 (see Table).

Flickering of the SP signal can cause not only thermal fluctuations of the particle potential. When measuring the height of the relief on the first pass in the resonant intermittent contact mode, the probe touches the particle for a small fraction of the period and can discharge it. It is possible to exclude such a touch by fixing the probe exactly above the particle, measuring the SP signal. For measurement times of hundreds of seconds, it will be necessary to minimize the drift in the probe–sample system. For example, the vertical drift seems to be < 0.01 nm/s.

The charges of the dielectric substrate, as discussed, create a long-range fluctuating field E_{SiO_2} Induced potential fluctuations $\sim E_{SiO_2}R$, i. e., they should grow with the particle size. However, in the experiment, the flickering potential decreases. Moreover, the signal noise above the dielectric (SP $\approx E_{SiO_2}h$, probe–sample distance $h \approx R$) is several times less than the potential flicker on the particle (see profiles in Figure 5, c).

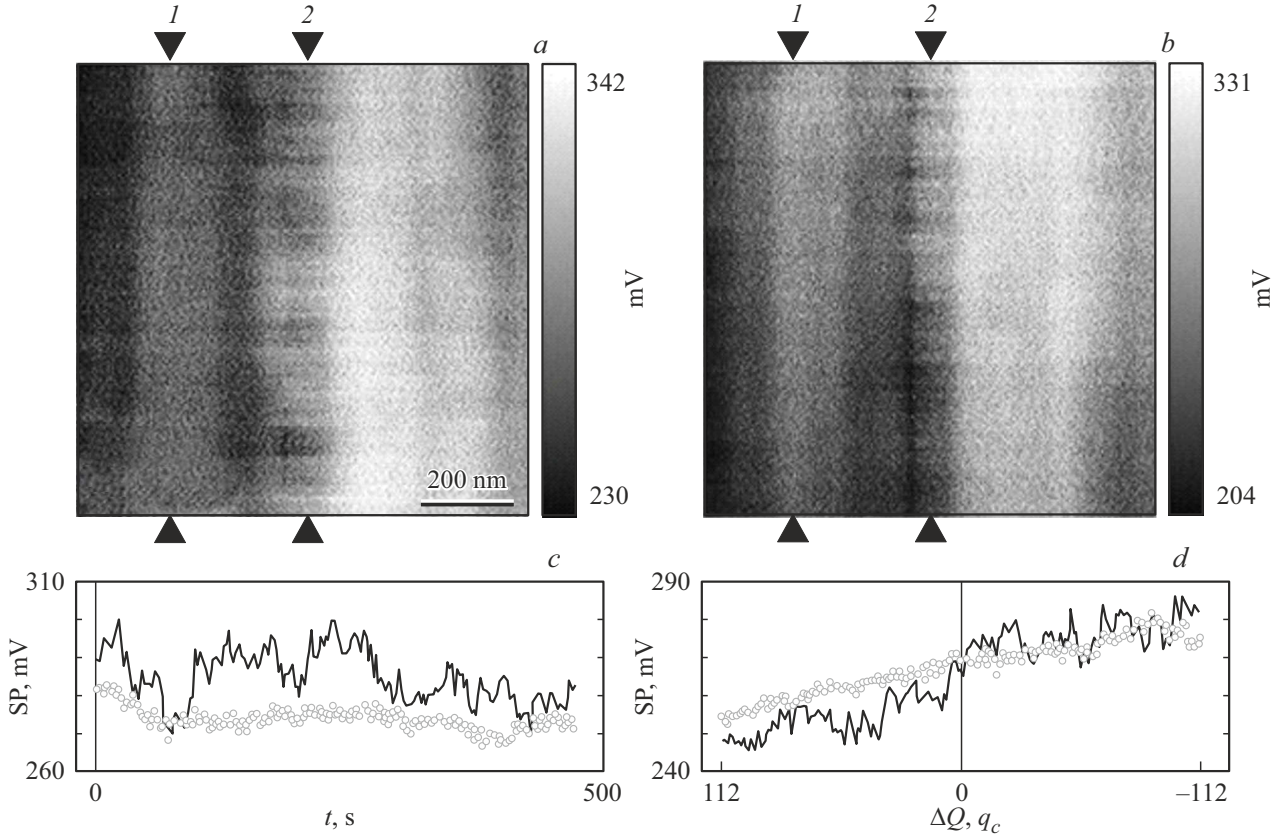

Figure 5. Repeated measurements of the SP signal along a single line through a 22-nanometer particle (No. 1, cantilever 1, see Table). a — $\Delta V = 0$; b — $d(\Delta V)/dt = 0.42$ mV/s (the hole was charged with an offset current ~ 0.5 e/s for 473 s). Profiles of the SP signal (time dependence) over a solid particle *2*, 300 nm to the left of its circle *1*: c — in the zero field; d — at the sweep.

A point charge Q can be trapped near a conducting particle, at a gap $-\delta$ from it. The potential near such a neutral particle has two contributions: the main one from the charge Q in the center of the sphere (particle model) and from the dipole $p = 2Q\delta$ [18]. The dipole contribution changes when the charge passes to other traps, but is small compared to the main one: at a distance of r from the trap, they are correlated as δ/r.

Spurious sources of scintillation of the SP signal from a conducting particle on a dielectric complicate the calibration of the SKPM signal by the amplitude of thermal fluctuations in the particle potential. However, there are different ways to determine PHV in the SKPM mode [5,14,20–22]. Using them will allow you to study the nature of flickering more deeply.

In Figure 5, *c* (profile of the „zero field" of the particle No. 1, $\sigma_0 = 6.3$ mV) the SP signal oscillates with a period of ~ 100 s and a drop of ~ 10 mV. The calculation of RMSV of the number of electrons for No. 1 using (8) gives $\sigma_{nQ} = 0.538$. Using this result, we obtain a response to 1*e*-a charge surge of $\Delta SP_{1e} = \sigma_0/\sigma_{nQ} \approx 12$ mV. Similarly, the values ΔSP_{1e} were obtained for particles No. 1, 4 and 6 (Figure 3, *b*–*d*): 18, 13 and 5 mV.

Compared to Figure 5, *c*, the profiles *1* and *2* in Figure 5, *d* grow on average by ~ 30 mV. This reflects changes in the edge field of the capacitor as ΔV grows at the lower contact during 473 from scanning (from bottom–upwards in Figure 5, *a* and *b*) from -100 mV to $+100$ mV at a rate of 0.42 mV/s (negative current $\leq 0.5\,e$/s; electrons charge the hole with a particle). In comparison with the zero field, the flicker on the profile of *2* in Figure 5, *d* goes out: $\sigma_- = 4.5$ mV, $\sigma_-0/\sigma_0 \approx 0.7$.

On the particle No. 4, the current ≤ 0.3 e/c led to $\sigma_-/\sigma_0 \approx 1.4$ and 1.2 (two different cantilevers); at No. 6 $\sigma_-/\sigma_0 \approx 1.5$, the current $\leq 0.8\,e$/sec. Y No. 3 currents $\leq 0.7\,e$/s (different signs), $\sigma_- = 8.2$ mV and $\sigma_+ = 6.0$ mV. As a result, the negative current enhances the flickering potential of the three particles, and only the smallest one quenches.

Flicker attenuation is similar to the suppression of thermal vibrations of a mechanical oscillator by a load that increases its rigidity. Indeed, thermal fluctuations in the potential can decrease (increase) if, when charging the hole, the capacity of the particle–substrate increases (decreases). On average, it drops at a negative current. According to (3) and (Clause 7), this capacity is small for small ε. There is usually a thin layer of atmospheric moisture on the substrate, $\varepsilon_{H_2O} = 81$. Such a composite substrate has an effective $\varepsilon > \varepsilon_{SiO_2} = 4$. Therefore, a drop (increase) in capacity may reflect desorption (adsorption) of water. Accordingly, the flickering of the particle potential will be amplified (attenuated) on a dry (wet) surface, which is interesting to test in an experiment.

4. Conclusion

Temporal fluctuations of the electrical potential of Au particles on the surface of a perforated contact of a capacitor structure based on *p*-Si with a thermal oxide 1.4 μm thick have been studied by scanning Kelvin probe microscopy in the amplitude modulation mode. Single particles with a height of 20–70 nm, located on the dielectric surface inside the contact microholes, had potential flickers with a RMS amplitude of ~ 10 mV and a frequency in the range of 0.01–0.1 Hz. The dependences of the amplitude of the flicker on the particle size and on the distance of the probe–particle are determined.

In the approximation of a conducting sphere on a dielectric, calculations of thermal fluctuations of the potential of a metal particle are carried out. A qualitative agreement of measurements with calculations has been obtained. The features of calibration of the SKPM signal of the surface potential on a nanometer thermal potential noise source are considered.

It remains to emphasize the following. The measured value of the fluctuations may be much less than the value predicted by statistical mechanics, since it is proportional to $(\tau/\Delta t)^{1/2}$, where $(2\pi\tau)^{-1}$ determines the width of the flat spectrum of thermal fluctuations, Δt is the value of the time constant of the device [23]. We believe that there is no such decrease in our case, since there are signal changes reflecting elementary charge surges on the particle. Indeed, the intervals τ between signal instabilities in Figures 2, 3, and 5 are greater than 10 s. In the presented data, a significantly shorter time passes between measurements of the potential over the particle $\Delta t \approx 2$ s (determined by the frequency of the line scan). The lifetime of the charge state of an Au particle, τ, is related to the Maxwell time of charge relaxation in the medium: $\tau_M = \varepsilon\varepsilon_0\rho$. Thermal silicon oxide is considered to be a very good insulator [24,25]. If, for example, $\rho_{SiO_2} \approx 10^{11}$–$10^{12}$ Ohm · m, then $\tau_M \sim 10$ s. By an order of magnitude, such relaxation times were found in AFM studies of the charge injection into samples of SiO_2–Si [26,27].

Acknowledgments

A.V. Ankudinov, A.M. Mintairov, V.D. Rodin, A.S. Schenin are supported by a grant from the Russian National Science Foundation SPbPF No. 24-22-20014.

Conflict of interest

The authors declare that they have no conflict of interest.

References

[1] R. Millikan. *Electrons (+ and −) Protons Photons Neutrons Mesotrons And Cosmic Rays* (M.–L., Gos. ob'edinen. nauch.-tekhn. izd-vo NKTP SSSR, 1939) ch. 5, p. 72. (in Russian).
[2] J.B. Zeldovich. UFN, **89**, 647 (1966). (in Russian).
[3] V.B. Braginsky. *Fizicheskie eksperimenty s probnymi telami* (M., Nauka, 1970) ch. 2, p. 76. (in Russian).
[4] M. Nonnenmacher, M.P. O'Boyle, H.K. Wickramasinghe. Appl. Phys. Lett., **58**, 2921 (1991).

[5] H.O. Jacobs, H.F. Knapp, A. Stemmer. Rev. Sci. Instrum., **70**, 1756 (1999).
[6] A. Tekiel, Y. Miyahara, J.M. Topple, P. Grutter. ACS Nano, **7**, 4683 (2013).
[7] Y. Zhang, O. Pluchery, L. Caillard, A.-F. Lamic-Humblot, S. Casale, Y.J. Chabal, M. Salmeron. Nano Lett., **15**, 51 (2015).
[8] Y. Abbas, M. Rezeq, A. Nayfeh, I. Saadat. Appl. Phys. Lett., **119**, 162103 (2021).
[9] B. Chatelain, A.E. Barraj, C. Badie, L. Santinacci, C. Barth. New J. Phys., **23**, 123009 (2021).
[10] D.V. Averin, K.K. Likharev. J. Low Temp. Phys., **62**, 345 (1986).
[11] G. Zimmerli, T.M. Eiles, R.L. Kautz, J.M. Martinis. Appl. Phys. Lett., **61**, 237 (1992).
[12] S.M. Verbrugh, M.L. Benhamadi, E.H. Visscher, J.E. Mooij. J. Appl. Phys., **78**, 2830 (1995).
[13] V.A. Krupenin, D.E. Presnov, M.N. Savvateev, H. Scherer, A.B. Zorin, J. Niemeyer. J. Appl. Phys., **84**, 3212 (1998).
[14] K.S. Ladutenko, A.V. Ankudinov, V.P. Evtikhiev. Pis'ma ZhTF, **36**, 71 (2010). (in Russian).
[15] A. Sommerfeld. *Elektrodinamika* (M., Izd-vo inostr. lit., 1958) ch. 2, p. 103 (in Russian).
[16] L.D. Landau, E.M. Lifshits. *Elektrodinamika sploshnyh sred* (M., Fizmatlit, 2005) ch. 1, p. 24. (in Russian).
[17] In. Smythe. *Electrostatics and Electrodynamics* (M., Izd-vo nostr. lit. 1954) ch. 5, p. 208. (in Russian).
[18] D.V. Sivukhin. **Elektrichestvo** (M., Fizmatlit, Izd-vo MFTI, 2004) ch. 1, p. 86. (in Russian).
[19] L.D. Landau, E.M. Lifshits. *Statisticheskaya fizika* (M., Nauka, 1976) p. 1, ch. 12, p. 363. (in Russian).
[20] U. Zerweck, C. Loppacher, T. Otto, S. Grafström, L.M. Eng. Phys. Rev. B, **71**, 125424 (2005).
[21] J. Colchero, A. Gil, A.M. Baro. Phys. Rev. B, **64**, 245403 (2001).
[22] A. Gil, J. Colchero, J. Gomez-Herrero, A.M. Baro. Nanotechnology, **14**, 332 (2003).
[23] D. McDonald. *Introduction to the physics of noise and fluctuations* (Moscow, Mir, 1964) ch. 1, p. 27. (in Russian).
[24] P. Burger, R. Donovan. *Fundamentals of Silicon Integrated Circuit Technology* (Moscow, Mir, 1969) vol. 1, part 1, ch. 3, p. 116. (in Russian).
[25] J.K. Srivastava, M. Prasad, J.B. Wagner, jr. J. Electrochem. Soc., **132**, 955 (1985).
[26] G.H. Buh, H.J. Chung, Y. Kuk. Appl. Phys. Lett., **79**, 2010 (1999).
[27] M.S. Dunaevskiy, P.A. Alekseev, P. Girard, E. Lahderanta, A. Lashkul, A.N. Titkov. J. Appl. Phys., **110**, 8 (2011).

Translated by A.Akhtyamov

Appendix

The potential of a charged conducting sphere lying on a dielectric

The problem is solved using the image method. Let's place the charge $Q_0 = 1$ in the center of the sphere at a height of R (see figure). The charge $-K$, its image in the dielectric at a depth of $-R$, will upset the equipotentiality on the surface of the sphere. The image of the charge $-K$ inside the sphere, the charge $K/2$ at a height of $R/2$, will restore it. Taking into account the next generations of images of charges in a dielectric and sphere, it is possible to obtain a solution in the form of an infinite series.

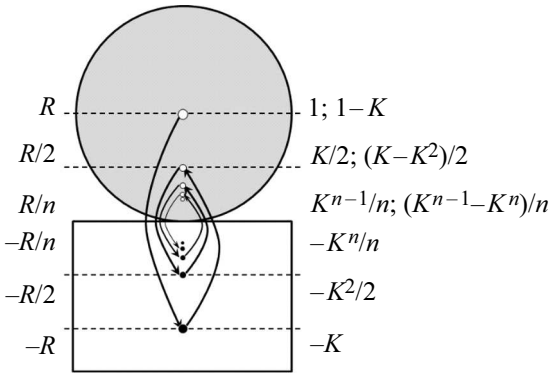

Infinite systems of point images of charges in a conducting sphere with radius R and in an insulator with dielectric constant ε; $K = (\varepsilon-1)/(\varepsilon+1)$. Outside the sphere, outside the dielectric, the potential is created by the systems of charges K^{n-1}/n inside the sphere and $-K^n/n$ in the dielectric; in the dielectric — the system $(K^{n-1}-K^n)/n$ inside the sphere.

Calculate the sum of all charges inside the sphere, Q:

$$Q = Q_0\left(1 + K/2 \ldots + K^n/(n+1)\ldots\right) = Q_0 \sum_{n=0}^{\infty} K^n/(n+1). \tag{A.1}$$

To do this, we note that

$$K^{n+1}/(n+1) = \int_0^K x^n dx, \tag{A.2}$$

and, since $K < 1$,

$$\sum_{n=0}^{\infty} x^n = 1/(1-x). \tag{A.3}$$

It follows from (A.2) and (A.3) that

$$K\sum_{n=0}^{\infty} K^n/(n+1) = \int_0^K dx/(1-x) = -\ln(1-K). \tag{A.4}$$

Combining (A.1) and (A.4), we obtain

$$Q = -Q_0\,\frac{\ln(1-K)}{K} = Q_0\,\frac{\varepsilon+1}{\varepsilon-1}\ln\frac{\varepsilon+1}{2}. \tag{A.5}$$

Let's place the center of the coordinate system in the center of the sphere in Figure 6, and point the axis Z upward. At $n \geq 2$, the charges K^{n-1}/n inside the sphere and $-K^n/n$ in the dielectric compensate for each other's potentials on the surface of the sphere, and only Q_0

contribute to the potential. Taking into account (*A*.5), we write

$$\varphi_{|r|=R} = \frac{Q_0}{4\pi\varepsilon_0 R} = \frac{(\varepsilon-1)Q}{4\pi(\varepsilon+1)\varepsilon_0 R\ln[(\varepsilon+1)/2]}. \quad (A.6)$$

Where do we get the expressions for the capacitance of a sphere on a dielectric:

$$C = 4\pi\,\frac{\varepsilon+1}{\varepsilon-1}\,\varepsilon_0 R\ln\frac{\varepsilon+1}{2} \quad (A.7)$$

and the electrostatic energy Φ of an isolated sphere with charge Q:

$$\Phi = \frac{Q^2}{2C} = \frac{Q\varphi_{|r|=R}}{2} = \frac{(\varepsilon-1)Q^2}{8\pi(\varepsilon+1)\varepsilon_0 R\ln[(\varepsilon+1)/2]}. \quad (A.8)$$

By entering $\mathbf{e}_Z$, a unit Z vector, we write down general expressions for the potential outside the sphere with charge Q:

$$\varphi_{z\geq -R} = \frac{(\varepsilon-1)Q}{4\pi(\varepsilon+1)\varepsilon_0\ln[(\varepsilon+1)/2]}$$

$$\times\left(\frac{1}{|r|}+\sum_{n=2}^{\infty}\frac{K^{n-1}}{|n\mathbf{r}+(n-1)R\mathbf{e}_Z|}-\sum_{n=1}^{\infty}\frac{K^n}{|n\mathbf{r}+(n+1)R\mathbf{e}_Z|}\right),$$

$$\varphi_{z\leq -R} = \frac{(\varepsilon-1)Q}{2\pi(\varepsilon+1)^2\varepsilon_0\ln[(\varepsilon+1)/2]}\sum_{n=1}^{\infty}\frac{K^{n-1}}{|n\mathbf{r}+(n-1)R\mathbf{e}_Z|}. \quad (A.9)$$